JAERI-M
87-102

DEVELOPMENT OF TOKAMAK REACTOR AUTOMATED DESIGN CODE "TRADE"

July 1987

Satoshi NISHIO, Tatsuzo TONE, Toshihide TSUNEMATSU,
Masao KASAI* and Masana NISHIKAWA*

日本原子力研究所
Japan Atomic Energy Research Institute

JAERI-Mレポートは，日本原子力研究所が不定期に公刊している研究報告書です。
入手の問合わせは，日本原子力研究所技術情報部情報資料課（〒319 11 茨城県那珂郡東海村）あて，お申しこしください。なお，このほかに財団法人原子力弘済会資料センター（〒319 11 茨城県那珂郡東海村日本原子力研究所内）で複写による実費領布をおこなっております。

JAERI-M reports are issued irregularly.
Inquiries about availability of the reports should be addressed to Information Division Department of Technical Information, Japan Atomic Energy Research Institute, Tokaimura, Naka gun, Ibaraki-ken 319-11, Japan.

編集兼発行　日本原子力研究所
印　　刷　日青工業株式会社

JAERI-M 87-102

Development of Tokamak Reactor Automated Design Code "TRADE"

Satoshi NISHIO, Tatsuzo TONE+, Toshihide TSUNEMATSU
Masao KASAI* and Masana NISHIKAWA*

Department of Large Tokamak Research
Naka Fusion Research Establishment
Japan Atomic Energy Research Institute
Naka-machi, Naka-gun, Ibaraki-ken

(Received June 22, 1987)

This report describes Tokamak Reactor Automated Design Code "TRADE" which has been developed in order to assess the impact of the design choices on reactor systems and to find out the optimum design concept through wide parameter range. The optimum design concept is realized by finding out the optimum compromise between the plasma performance, the torus structure and the coil systems. Furthermore, TRADE code is for producing an input data set into TORSAC which had already been developed for a sensitivity analysis.

Keywords: Tokamak Reactor, Conceptual Design, Plasma Performance, Optimization, ANISN, MHD Equilibrium, Objective Function

+ Office of Planning
* Mitsubishi Atomic Power Industries (MAPI), INC

JAERI－M 87－102

トカマク炉の自動設計コード“ＴＲＡＤＥ”の開発

日本原子力研究所那珂研究所臨界プラズマ研究部

西尾　敏・東稔達三[+]・常松俊秀・笠井雅夫[*]・西川正名[*]

（1987年6月22日受理）

原研と三菱原子力工業㈱との共同研究としてトカマク炉の自動設計コード（ＴＲＡＤＥ）が開発された。本コードはプラズマとトーラス構造体およびコイルシステム間の整合性をとりつつ最適炉概念を構築するものである。最適化はコード内にオプションとして用意されている幾つかの評価関数に従ってなされる。また本コードは既に開発されているトカマク炉システムの解析・評価コード“ＴＯＲＳＡＣ”の入力データ作成コードとして位置付られるものである。

那珂研究所：〒311-02 茨城県那珂郡那珂町大字向山801－1
＋企画室
＊三菱原子力工業㈱

Contents

目　　次

1. Introduction

The Research and development (R&D) of the controlled thermonuclear fusion as an ultimate energy source has a long history. Many confinement types have been studied and tokamaks are the most representative. Examining the R&D activities of the past, we notice that efforts for machine construction have been rapidly increasing and this tendency will be continued in the future. A tokamak system utilizes many physical principles and technologies. Nuclear physics, plasma physics, electromagnetics, thermodynamics, mechanics and so on are complexly combined in tokamak design and many high technologies such as superconductivity, ultra-high vacuum, high heat removal technology and advanced materials are required.

This extreme complexity of design has the consequence that a small modification of a part of the design has a potential to be reflected in many parts of design in many respects. Furthermore, this feature suggests the difficulty in design optimization because the formation of a self consistent tokamak design and the evaluation of its characteristics are troublesome and require the expenditure of a large amount of professional staff design time. We should note that the scale and complexity of the tokamak has been increasing and this tendency will continue until the completion of the commercial tokamak reactor. The construction period and investment has appreciably expanded even for the present-day tokamaks. Thus, it is sufficiently profitable to go to the expence of improving the accuracy in design calculation in order to reduce the design redundancy.

There has been a growing demand for a computer code which performs a systematic analysis of overall reactor systems. We had developed the computer code named TORSAC[1,2] (Tokamak Reactor System Analysis Code) during past several years. We take a "reference design learning method" for TORSAC. A set of the reference design parameters, which resembles the objective tokamak concept, is put into TORSAC at first, and then TORSAC constructs an arbitrary tokamak design image consistently based on the reference design. TORSAC does not have a function to produce a new design concept without preparing a reference design beforehand. In effect, TORSAC does not perform an automatic design optimization. In this meaning, the "S" in TORSAC seems to be rather "S" of sensitivity than "S" of system.

With this mind, the function of an automatic design optimization is indispensable for producing a new design concept. We have been developing a code named TRADE (Tokamak Reactor Automated Design Code) side by side with TORSAC. The positioning of TRADE Code is a charcterized code for producing an input data set into TORSAC. The so-called design activity is the process of inquiring the best design point under the given design condition. The automated design code should include a function of the optimization. Therefore, the design calculation should be iterated so far as a convergence according to the objective function. Most objectives will be normally minimized (e.g. plasma size, PF coils ampere turns, capacities of the auxiliary components and etc.) or maximized (e.g. plasma performance, obtainable volt-seconds from PF coils and etc.) as appropriate.

In Chapter 2, we describe outline and over all structure of TRADE code. In Chapter 3, the method and model for analysis are described.

2. Outline and Structure of TRADE Code

The tokamak device is at any rate an electrical equipment, and its fundamental concept might be firstly defined by the plasma performance and the magnetic coil systems. The specifications of other components will be resultantly decided. Therefore, the major efforts should be made in the optimization process of the plasma design and the coil systems design (especially, PF coil system). The stratum of the required information or data for calculating the basic machine parameters is schematically shown in Fig. 2.1.1.

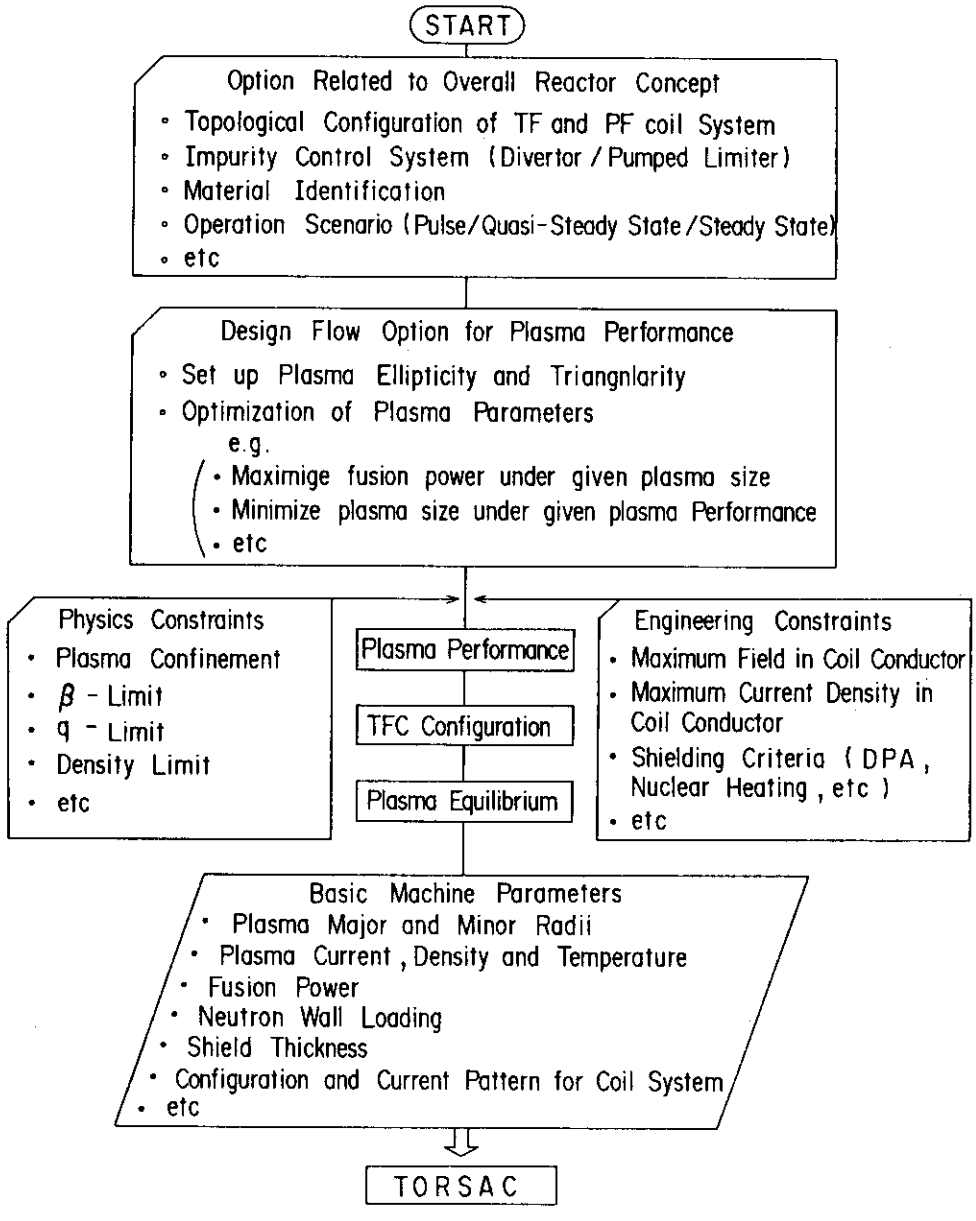

Fig. 2.1.1 Schematic Stratum of Design Calculation

3. Method and Model for Analysis

3.1 Design of Plasma Physics

3.1.1 Basic consideration and Eeature

It is important to know what kinds of physics and engineering constraints have influence on the determination of plasma parameters satisfying a required performance or a design objective. In TRADE, the engineering constraints (e.g neutron wall loading, plasma elongation, radiation shielding condition etc.) are not used for a determination of plasma parameters, but are used the design conditions for a determination of specifications of the associated components. The key constraints for plasma physics are energy confinement time, safety factor, density limit and beta limit.

i) Energy Confinement Time

Several option of confinement models have been incorporated to describe conduction losses. The ions are treated with the neoclassical formulation, and the electrons are treated with empirical scaling, such as Alcator, Neo-Alcator, Goldston (L-mode), Gill (H-mode) and Mirnov. They are listed in Table 3.1.1

Table 3.1.1 Scaling law option for energy confinement time

• Energy Confinement Time			
Ion	1	• $\tau_{Ei} = C_{Ei} \cdot 4.7 \times 10^{18} \dfrac{B_o^2 \sqrt{T_i}\, a_p^2}{A^{1.5} n_i q_\psi^2}$	Neo-classical
Electron	1	• $\tau_{Ee} = C_{Ee} \cdot 1.1 \times 10^{-20} n_e a_p^2$	Alcator
	2	• $\tau_{Ee} = C_{Ee} \cdot 1.15 \times 10^{-21} n_e a_p^{0.8} R^{2.3}$	Neo-Alcator
	3	• $\tau_{Ee} = \dfrac{(\tau_{Ee}^A \cdot \tau_e^B)}{(\tau_{Ee}^A)^2 + (\tau_{Ee}^B)^2}$ $\tau_{Ee}^A = C_{Ee} \cdot 1.03 \times 10^{-21} n_e a_p^{1.04} R_p^{2.0} R_p^4 q_\psi^{0.5}$ $\tau_{Ee}^B = C_{Ee} \cdot 3.68 \times 10^{-5} I_p P^{-0.5} R^{1.75} a_p^{-0.37} \kappa^{0.5}$	Goldstone(L-mode) p_h:Heating power
	4	• τ_{Ee} : 2 × Goldstone (L-mode)	Goldstone(H-mode)
	5	• $\tau_{Ee} = C_{Ee} \cdot 9 \times 10^{-27} I_p^{-0.61} n_e^{1.33} T_e^{0.75} R_p^{0.82} Z_{eff}^{0.07}$	Gill (H-mode)
	6	• $\tau_{Ee} = C_{Ee} \cdot 1.45 \times 10^{-7} a_p I_p$	Mirnov

$Z_{eff} = (1 + f_z \cdot Z^2)/(1 + f_z \cdot Z)$

f_z: ratio of the impurity ion density n_I to fuel ion density $(=n_I/n_i)$

ii) Safety factor limit

In general, MHD equilibrium calculations are carried out to accurately model the plasma current (and, in turn, true MHD safety factor q_ψ) dependence on plasma (κ, δ) and aspect ratio ($A=\frac{R}{a}$). A fit to these model equilibriums can be characterized as

$$q_\psi = q_a\left[\,1 + \frac{f_1(\delta)}{\sqrt{A}}\,\right]\left[1 + \frac{\beta_p\, f_2(\delta)}{A^{1.5}}\,\right]^{3)} \qquad (3.1.1.)$$

where

$$q_a = \frac{2\pi}{\mu_0}\,\frac{aB_0}{I_p\,A}\,\frac{1+\kappa^2}{2}$$

$$f_1(\delta) = 0.16 + 0.633\,\delta$$

$$f_2(\delta) = 2.45 + \delta$$

B_0 = toroidal field on plasma axis

or

$$1/q_\psi = A\sqrt{\left(1 - \frac{1}{A^2}\right)}\left(\frac{2}{1+\kappa^2} - 0.08\,\delta\right)\frac{\mu_0 I_p}{2\pi a B_0} - 0.07\left\{1+(\kappa-1)\delta\right\}^{3)} \qquad (3.1.2)$$

From the requirement of the MHD stability (tearing mode), around 2.5 of q_ψ is often employed in the plasma design.

iii) Density limit

In many tokamaks, the maximum density attainable in stable operation is seen to scale as B_0/R, known as the Murakami limit[4],

$$n_{max} = \nu\,\frac{B_0}{q_\psi\,R} \times 10^{20}\ (m^{-3}) \qquad (3.1.3)$$

where $\nu \simeq 1.5$ for ohmically heated plasma, and $\nu \simeq 2 \sim 3$ is found to be possible in some auxiliary heated plasma.

iv) Toroidal Beta Limit

As a general manner, toroidal beta limit is merely called beta limit. The specific limits on this beta value that have been incorporated are those proposed by Bernard[6], Tuda[3] and Troyon[7], and are left to a user's option. The are listed in table 3.1.2.

Table 3.1.2 Scaling law option for beta limit

Toroidal Beta Limit			
BETA	1	$\cdot \beta_{max}=C_\beta \cdot 7.8\times10^{-2}\, q_\psi^{-0.54}(A-1)^{0.75}\kappa^{1.014}(q_\psi-1)$	Tuda
	2	$\cdot \beta_{max}=C_\beta \cdot \frac{0.3\kappa^{1.5}}{Aq_\psi}\{1+0.9(\kappa-1)\delta-0.6\frac{\kappa^{0.75}}{q_\psi} + 14(\kappa-1)(1.85-\kappa)\frac{\delta^{1.4}}{q_\psi^4}\}$	
	3	$\cdot \beta_{max} = C_\beta \cdot 0.23 \frac{\kappa^{1.2}}{A^{1.3}\, q_\psi^{1.1}}(1+1.5\delta)$	Bernard
	4	$\cdot \beta_{max} = C_\beta \cdot 3.5 \times 10^{-6} \frac{I_p}{a_p\, B_o}$	Empirical

v) Poloidal Beta Limit and Operation Range

A uniform magnetic field in the vertical direction.

$$B_\perp = -\frac{\mu_o\, I_p}{4\pi R}\left(\ln\frac{8R}{a} + \Lambda - \frac{1}{2}\right) \qquad (3.1.4)$$

must be applied in order to maintain a toroidal plasma with circular cross section in equilibrium state[8], where

R : Plasma major radius

a : Plasma minor radius

I_p: Plasma current

$$\Lambda = \beta_p + \frac{\ell_i}{2} - 1 \qquad (3.1.5)$$

and β_p and ℓ_i are the poloidal beta and the internal inductance of the unit length of plasma column respectively. The direction of $B_\perp$ is opposite to that of the field due to the plasma current inside the torus, so that the resultant poloidal field becomes zero at some point inside the torus and a separatrix is formed. When the plasma pressure is increased and β_p becomes large, the required $B_\perp$ is increased and the separatrix shifts toward the plasma. The upper limit of the plasma pressure is determined by the condition that the resultant poloidal field at r=R-a on the midplane is zero. Under the assumption of uniform plasma pressure, surface current and a/R << 1, the upper limit β_p^c of the poloidal beta is

$$\beta_p^c = \frac{\pi^2}{16}\frac{R}{a} \approx 0.5\,\frac{R}{a} \quad [8] \,. \qquad (3.1.6)$$

Thus the upper limit of β_p^c is half of the aspect ratio R/a, the required equilibrium field for a non-circular plasma is composed of not only vertical (dipole) field but also quadrapole and hexapole field. The equilibrium field for an elliptic plasma has a negative decay index (negative n-value), because the vertical field is decreased by the quadrapole field inside the torus. In the case of an elliptical cross-section, the upper limit β_p^c of the poloidal beta is proportional to $(1 + \frac{1}{2}\varepsilon)$ [11], where $\varepsilon = (\kappa^2 - 1)/(\kappa^2 + 1)$ and κ is ellipticity.

However it is finally to be certified by the equiriblium calculation whether the designed plasma parameters are allowable or not, we use the following expression as a provisional β_p^c. [10]

$$\beta_p^c \leq \frac{A}{2}\left\{1 + \frac{1}{2}\left(\frac{\kappa^2 - 1}{\kappa^2 + 1}\right)\right\} \qquad (3.1.7)$$

Next we discuss an operation range of the poloidal beta in relation to a toroidal beta β and a stability condition.

At first, we set up an attainable β_p in relation to the toroidal beta β. For simplicity of analysis the upper limit β_{max} of the toroidal beta is represented by Troyon scaling[7] listed in Table 3.1.2. C_β of unity corresponds with C_f of 17.5.

$$\beta_{max} = C_f \frac{\mu_2 I_p}{2\pi a B_o} \quad (\%) \tag{4.1.8}$$

The geometrical safety factor, q* is

$$q^* = \frac{2\pi a^2 B_o}{\mu_o I_p R} \frac{1+\kappa}{2} \tag{3.1.9}$$

The poloidal beta, β_p is expressed as

$$\beta_p = \frac{2\mu_o \langle P \rangle}{B_p^2} \quad , \tag{3.1.10}$$

where $\langle P \rangle$ is plasma average pressure and B_p $\left(= \frac{\mu_o I_p}{2\pi a \sqrt{\frac{1+\kappa^2}{2}}}\right)$ is poloidal field at the plasma surface produced by the plasma current.
The toroidal beta, β is expressed as

$$\beta = \frac{2\mu_o \langle P \rangle}{B_o} \times 100 \quad (\%) \ , \tag{3.1.11}$$

Form the formulas of (3.1.6), (3.1.7) and (3.1.4), we obtain

$$\frac{1}{100} \cdot \frac{\beta}{\beta_p} = \left(\frac{\mu_o I}{2\pi a B_o} \right)^2 \frac{2}{1+\kappa^2} = \beta_{max}^2 \cdot \frac{2}{1+\kappa} \ . \tag{3.1.12}$$

When β value takes the β_{max}, we obtain

$$\beta_p^c \cdot \beta_{max} = \frac{1}{100} \cdot C_f^2 \frac{1+\kappa^2}{2} \ . \tag{3.1.13}$$

If C_f is replaced by C_β, we obtain

$$\beta_p^c \cdot \beta_{max} = 1.03 \cdot C_p^2 (1+\kappa^2)$$

There, the allowable range for β_p is

$$\beta_p \leq \frac{1.03}{\beta_{max}} \cdot C_\beta^2 \cdot (1 + \kappa^2) \tag{3.1.14}$$

On the other hand, from the formulas of (3.1.5) and (3.1.8), we obtain

$$\frac{1}{100} \cdot \frac{\beta}{\beta_p} \left(\frac{\mu_0 I_p}{2\pi a B_T} \right)^2 \frac{2}{1 + \kappa^2} = \frac{1}{(q^* A)^2} \cdot \frac{1 + \kappa^2}{2} \tag{3.1.15}$$

The stability condition called Kruskal-Shafranov condition requires the safety at the plasma center be more than unity and correspond to 2 or 3 at the plasma boundary (surface). Thus the safety factor q^* has a lower limit value q_c^* around 2 or 3 ($q^* \geq q_c^*$). Therefore the formula (3.1.11) becomes

$$\beta_p \geq \frac{\beta}{100} (q_c^* A)^2 \frac{2}{1 + \kappa^2} \quad . \tag{3.1.16}$$

Thus from the formulas (3.1.7), (3.1.14) and (3.1.16) the operation range is schematically showed in Fig. 3.1.1.

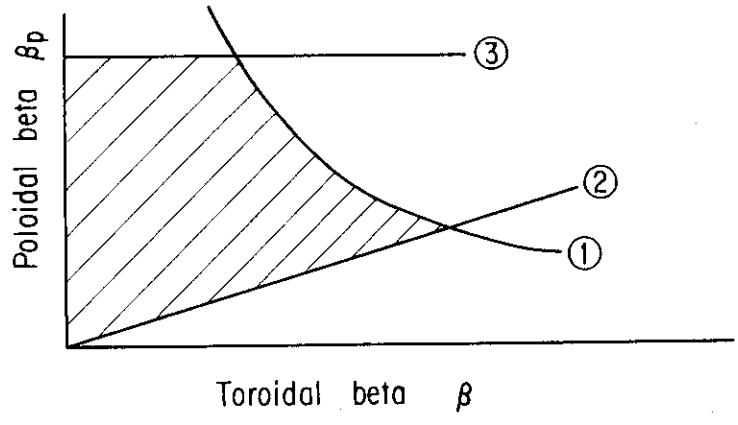

Fig. 3.1.1 Operation range in $\beta - \beta_p$ space, ① $\beta_p \beta = 1.03\ C_\beta (1+\kappa^2)$, ② $\beta_p = \frac{\beta}{100} (q_c^* A)^2 \frac{2}{1+\kappa^2}$, ③ Limit or existence of equiriblium solution. (provisional β_p^c is $\frac{A}{2}\left\{1 + \frac{1}{2}\left(\frac{\kappa^2-1}{\kappa^2+1}\right)\right\}$). Where, C_β, κ, q_c^* and A are modefied coefficient to Toroyon scaling, plasma elongation, lower limit of safety factor at plasma boundary and aspect ratio, respectively.

vi) Plasma power balance

The plasma power balance is a zero-dimensional representation with plasma temperature and density profile effects and is expressed by the following equations including a two-fluid model of the electron and ion.

For electron

$$\frac{dW_e}{dt} = G_e P_\alpha + H_e P_\kappa + R_e P_{rf} + P_J - P_{xe} - P_{sy} - P_{br} - P_{ei} - P_{imp} \qquad (3.1.13)$$

For ion

$$\frac{dW_i}{dt} = (1-G_e)P_\alpha + (1-He)P_h + (1-R_e)P_{rf} + P_{ei} - P_{xi} - P_{cx} \qquad (3.1.14)$$

where

W_e : electron thermal energy
w : ion thermal energy
G_e : fraction of α-particle energy to the electrons
P_α : α-particle heating
H_e : fraction of NBI energy to the electrons
P_h : NBI heating (including current drive)
R_e : fraction of deposited RF power to the electrons
P_{rf} : deposited RF power (including current drive)
P_J : joule heating induced by PF coil system
P_{xe} : transport energy loss of the electrons
P_{sy} : synchrotron radiation loss
P_{br} : bremsstrahlung radiation loss
P_{ei} : electron-to-ion energy relaxation rate
P_{imp} : radiation loss by impurities
P_{xi} : transport energy loss of the ions
P_{cx} : charge exchange loss

When the electron and the ion have a common temperature, a steady-state power balance is expressed by following simple equation.

$$P_\alpha + P_w + P_{rf} + P_J - P_{xe} - P_{xi} - P_{sy} - P_{br} - P_{imp} - P_{cx} = 0 \qquad (3.1.17)$$

For G_e, we use the following simple expression.[12)]

・ $G_e = (1 - \bar{T}_e/1.5 \times 10^5)^2$

・ $P_\alpha = \frac{1}{4} n;\ \langle\sigma v(T)\rangle \cdot E_\alpha \cdot f_\alpha \cdot \alpha_{eff}$

$\langle\sigma v(T)\rangle$, E_α, f_α and α_{eff} are the rate coefficient for D-T fusion reactions, the energy of produced α-particle, the correction factor representing the effect of the density and temperature profile on fusion power production, and the heating efficiency by α-particles.

where $\langle\sigma v(T)\rangle$: $10^{-22} \exp\{a_1(\ln T_i/1000)^3 + a^3(\ln T_i/1000)^2 + a_3(\ln T_i/1000) + a_4\}$ --- for $T_i \geq 1000$ eV

$a_1 = 0.038245$

$a_2 = -1.0074$

$a_3 = 6.3997$

$a_4 = -9.75$

$\langle\sigma v(T)\rangle = 0$ --- for $T_i < 1000$ eV

$E_\alpha = 3.52 \times 10^6$ eV $= 5.639 \times 10^{-13}$ Joule,

$$f_\alpha = 2 \int_0^1 n(\alpha)^2 f(T(\alpha)) \alpha d\alpha \ / \ \bar{n}^2 f(\bar{T})$$

where, $\alpha = r/a_p$

$f(T) = \langle\sigma v(T)\rangle$

$T(\alpha) = T_{io}(1 - \alpha^{NT})^{MT}$

$n(\alpha) = n_{io}(1 - \alpha^{ND})^{MD}$

$\bar{T} = \int_0^1 T(\alpha) \cdot 2\alpha \, d\alpha$

and $\bar{n} = \int_0^1 n(\alpha) \cdot 2\alpha \, d\alpha$

and

$\alpha_{eff} = 1.0 - 0.04 \exp(\gamma)$ --- A $I_p \geq 7.5 \times 10^6$

$= 0$ --- A $I_p < 7.5 \times 10^6$

where, γ : toroidal ripple (%).

・ $H_e = 1 - f_i$

Where, f_i is the fraction of energy recieved by ions, expressed of the following formula[12] and shown in Fig. 3.1.2.

$$f_i = \frac{2}{h}\left[-\frac{1}{6}\ln\left\{\frac{(1+\sqrt{\kappa})^2}{\kappa-\sqrt{\kappa+1}}\right\}+\frac{1}{\sqrt{3}}\arctan\left(\frac{\sqrt{3}\sqrt{k}}{2-\sqrt{\kappa}}\right)\right],$$

$$\text{where } \kappa = \frac{A^{2/3}}{14.6\,A_b}\,\frac{E_o}{T_e}$$

E_o : beam energy

A_b : atmic weight of NBI particle

$$A = (1-f_z)(2f_D + 3f_T) + 2f_z Z$$

where f_D : fraction of dutrium

f_T : fraction of tritium

f_z : fraction of (z) impurity

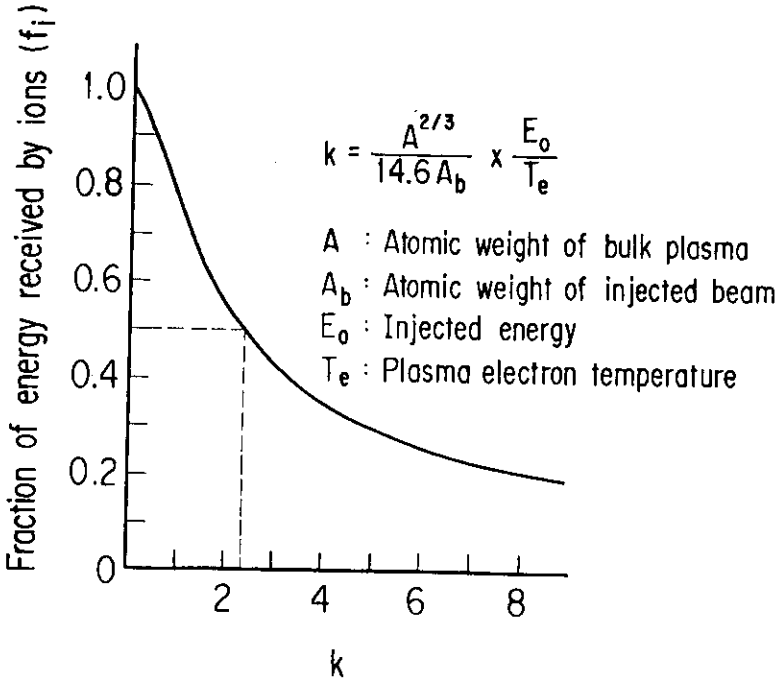

Fig. 3.1.2 Fraction of injected particle energy conveyed to the plasma ions versus the injected particle energy expressed in normalized units.

・ $R_e = 1$ --- ECW, LHW, CAW
$= 0$ --- ICRW

・ P_{rf} (in case of current drive by rf)

$P_{rf} = j_{rf} \cdot 5.38\times10^{-14}\, n_e/n_z T_e^{3/2}$ --- CAW

n_z : parallel refractive index

$P_{rf} = j_{rf} \cdot 1.127 \times 10^{-15} \cdot n_e\, G/T_e$ --- LHW

$$G = \frac{\ln(1+\tilde{\delta})}{C_f^2\, \tilde{\delta}\, (\tilde{\delta}+2)}$$

$$\tilde{\delta} = \frac{238.5}{T_e - 1}$$

$$C_f V_e = \frac{C}{n_{z1}} \quad --- \quad C_f = 3 \quad (C;\ \text{light velocity})$$

n_{z1} : upper parallel refractive index
v_e : electron thermal velocity

$$j_{rf} = \frac{I_{rf}}{\pi\, a_p^2\, \kappa}$$

where, I_{rf} is plasma current driven by rf.

・ $P_J = \eta\, j_{OH}^2$

$\eta = 3.0 \times 10^{-3}\, Z_{eff}\, \bar{T}_e^{-1.5}$

$Z_{eff} = 1 + f_z\, Z^2$

$j_{OH} = I_p/S_p$

$S_p = \pi a_p^2 \kappa$

・ $P_{xe} = 1.5\, \kappa\, n_e\, T_e/\tau_{Ee}$

$\kappa = 1.602\times10^{-19}$ Joule/eV

τ_{Ee}: electron energy confinement time in accordance with a scaling law option

・ $P_{sy} = 6.38\times10^{-16}\, B_o^{2.5}\, T_e^2\, \left(\frac{n_e}{a_p\, A}\right)^{1/2}$

B_o : toroidal field strength (tesla)

$A = \frac{R_p}{a_p}$

- $P_{br} = 1.41 \times 10^{-38} Z_{eff} n_e^2 \sqrt{T_e}$

- $P_{ei} = \frac{1.5 n_e (T_e - T_i) \kappa}{\tau_{ei}}$

$$\tau_{ei} = 4.38 \times 10^{13} Z_{eff} \frac{T_e^{1.5}}{n_e}$$

$\kappa = 1.602 \times 10^{-19}$ Joule/ev

- $P_{imp} = (f_z \cdot n_e^2 \cdot 10^{0.769[\log_{10} \frac{T_e}{4\times10^3}]^2} - \frac{P_{br}}{Z_{eff}} \cdot Z^2 f_z$

f_z: ratio of the impurity ion density n_I to fuel ion density ($=n_I/n_I$)

- $P_{xi} = 1.5 \kappa n_i (1 + f_z) T_i / \tau_{Ei}$

τ_{Ei}: ion energy confinement time (Neo-classical)

- $P_{cx} = 1.5 \kappa n_i n_o \langle \sigma v \rangle_{cx} (T_i - T_o)$

3.1.2 Computation logic and option

The plasma physics model used in TRADE includes a two-fluid model of the electron-ion power balance and a comprehensive treatment of the confinement modeling as mentioned before. A set of the plasma parameters is calculated subject to constraints imposed by the machine configuration and plasma equilibrium, stability, and confinemnet.

The physics module can operate in 13 modes (design flow options). The plasma performance may be determined for a specified machine configuration, or the device parameters may be computed for a given performance criterion. For example, one of 13 design flow options is to give a ignition margin (fusion alpha power/plasma power loss) and a plasma burning time as performance criteria, and plasma temperature, density and major dadius are to be calculated under as optimization condition of minimum minor dadius. A set of parameters satisfying the physics constrains usually necessitates iteration between the physics module and the other modules. The thirteen plasma design flow options prepared in TRADEC are listed in Table 3.1.3.

Table 3.1.3 Plasma Design Flow Option

Option No.	Assingned Parameters	Calculated Parameter	Optimization Condition (Objective Function)
1.	R_{TC} , Q	n, T	Minimum a
2.	R , Q	n, T	Minimum a
3.	R_{TC} , P_W	n, T	Minimum a
4.	R_{TC} , a	n, T	Maximum P_f
5.	R_{TC} , a	n, T	Maximum Q
6.	R , a	n, T	Maximum P_f
7.	R , a	n, T	Maximum Q
8.	R , a, Q	n, T	------
9.	R , T	n, a	Maximum P_f
10.	R , T	n, a	Maximum Q
11.	R_b , Q	n, T, R	Minimum a
12.	T_s , Q	n, T, R	Minimum a
13.	T_b , I_g	n, T, R	Minimum a

where

n : Plasma density
T : Plasma temperature
Q : Energy multiplication factor
P_W : Neutron wall loading (MW/m^2)
P_f : Fusion Power
T_b : Burn time (sec)
T_s : Plasma resistive skin time ($=1.8ka^2T_e^{3/2}$) (sec)
I_g : Ignition margin (fusion alpha power/plasma power loss)
R_{IC}, R, a: See Fig. 3.3.1

A mathematical method for optimization is applied as follows. In a steady-state (e.g. plasma burning phase), both of dW_e/dt and dW_i/dt in eq. (3.1.13) and (3.1.14) become zero. From eq. (3.1.14), we get

$$P_h = (1-He)^{-1}[P_{xi}-P_{ei}-(1-G_e)]P_\alpha \quad ,$$

and we substitute this P_h for left term of eq.(3.1.13), then we make a following function where, n_i, T_i and a are independent variables.

$$F(n_i,T_i,a)=G_eP_\alpha + H_e(1-He)^{-1}[P_{xi}-P_{ei}-(1-G_e)P_\alpha]$$

$$+ P_{rf} + P_J - P_{xe} - P_{sy} - P_{br} - P_{ei} - P_{imp} \qquad (3.1.16)$$

The electron temperature T_e and density n_e are eliminated in accordance with the following equations.

$$n_e = n_i\ (1 + Z\ f_z)$$

$$n_eT_e + (n_i + n_i\ f_z)T_i = \frac{B_o^2}{2\mu_o\kappa}\ \beta_{max}$$

where

Z : charge of the impurity

f_z : ratio of the impurity ion density n_I to fuel ion density ($= n_I/n_i$)

i) In cases of option 1, 2, 3, 8, 12 and 13

These cases require solving an equation system which consists of $F(n_i, T_i, a)=0$ and one of the following equations.

$$P_f\ (n_i, T_i, a) = 5\ P_\alpha\ (n_i, T_i, a)$$

or

$$Q(n_i, T_i, a) = P_f/(P_h/P_{rf})$$

or

$$I_g=P_\alpha/(P_{xe}+P_{sy}+P_{br}+P_{in}+P_{cx})$$

or

$$P_w=4\ a\ P_\alpha/(2\sqrt{1+\kappa^2/2})$$

For the numerical solution, a is started from zero and we find the minimun a where a set of n_i and T_i satisfy the above mentioned equation system by Newton-Raphson method of two variables.

As an example, we show the flowchart of the option 13 in Fig. 3.1.3.

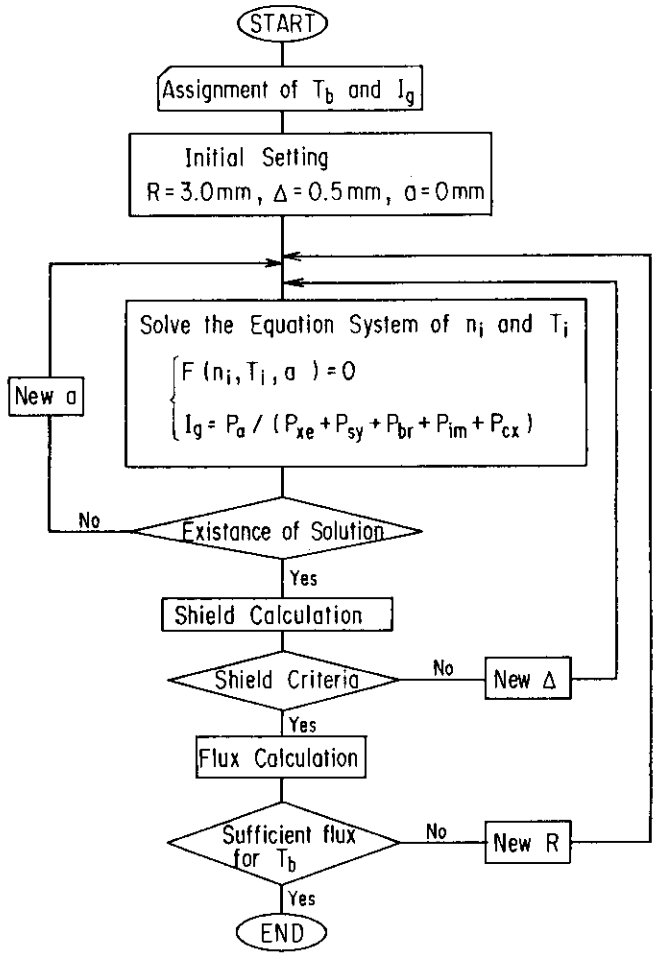

Fig. 3.1.3 Flowchart of option 13

ii) In cases of option 4, 5, 6, 7, 9, 10

This is a problem to maximize Q or P_f under a constraint condition $F(n_i, T_i, a) = 0$. For the numerical solution, a non-linear optimization methods[14,15,16], which is the flexible tolerance method is introduced.

3.2 Design of Radiation Shield

3.2.1 Basic Consideration Feature

In the tokamak fusion reactor which produces energetic neutrons, radiation shield is an important component because it not only determines the overall size of the reactor but it also influences the repair and maintenance scheme. Since huge amount of the shielding materials will be required, the optimization of the shield thickness becomes necessary. As shown in Fig. 3.2.1 a simplified model of a tokamak reactor is used for determining the shield thickness. This model forms concentric multi-layered and infinite cylindrical structure.

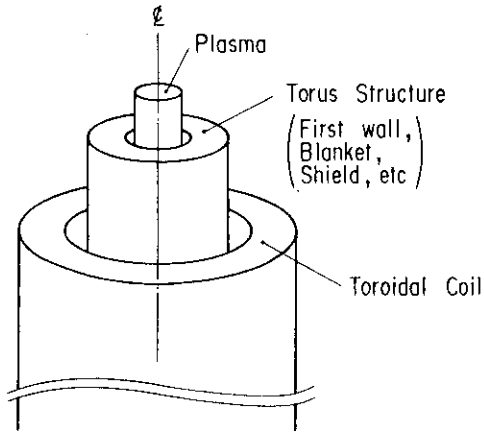

Fig. 3.2.1 Tokamak model for shield calculation

The D-T neutrons are uniformly generated in the plasma region. The one-dimentional discrete ordimate transport code ANISN[17] is used with the P_5-S_8 approximation for the radiation transport calculation. The 42-group neutron and 21-group gamma ray coupled cross section set GICX40[18] is used. The shielding responses (nuclear heating, DPA, absorbed dose, etc.) of magnets (composed of stainless steel, superconducting material copper, organic insulator, etc.) are calculated by using APPLE-2[19] code.

3.2.2 Computation logic and option

The infinite cylindrical structures model shown in Fig. 3.2.1 should be modelled to adopt ANISN input format. A rewritten model is shown in Table 3.2.1.

Table 3.2.1 Preparation for Shield Calculation

e.g. Radial build	℄ Plasma, Void, Coolant, Blanket wall, Blanket, Void, Shield, Cryostat, TFC can, TFC, Void, PFC can, PFC
Zone No.	1 2 3 4 5 6 7 8 9 10 11 12 13 14 15 ----------
Zone thickness (m)	0 Δ_1 Δ_2 Δ_3 Δ_4 Δ_5 Δ_6 Δ_7 Δ_8 Δ_9 Δ_{10} Δ_{11} Δ_{12} Δ_{13} Δ_{14} Δ_{15} ----------
Number of mesh	N_1 N_2 N_3 N_4 N_5 N_6 N_7 N_8 N_9 N_{10} N_{11} N_{12} N_{13} N_{14} N_{15} ----------
Zone No. with variable thickness (None or only one)	e.g. No. 7
Material No. and composition ratio	(see below)

Zone No.	1	2		3	4					k			
Material No.*	99	3	29	3	3	23	27	29	64	M_a	M_b	M_c	-------
Composition ratio	1.0	0.3	0.7	1.0	0.23	0.11	0.6	0.05	0.01	r_a	r_b	r_c	-------

$r_a + r_b + r_c + \cdots\cdots = 1.0$

* Material table is prepared in Appendix (e.g. Material No. 27 is Li_2O)

When an option of the optimization for the shield thickness is chosen, the thickness of the variable zone (Δk) is changed in accordance with the following formula.

$$\gamma^C = \mathrm{MAX}\left\{DPA^C/DPA^S,\ H_n^C/H_n^S\right\}$$

$$\Delta_k' = \Delta_k + \delta_{10} \log_{10} \gamma^C$$

where

DPA^C : Calculated value of DPA (displacement per atom)

DPA^S : Criterion for DPA

H_n^C : Calculated value of neuclear heating

H_n^s : Criterion for nuclear heating

δ_{10} : An increase in shield thickness for reducing neutron flux one order the magnitude

Here, we define Δ according to following formula for characterizing the radial build.

$$\Delta = \sum_{i=1}^{N_\Delta} \Delta_i$$

where, N_Δ is the component number of just before the TF coil conductor.

The computation logic for shield design is shown in Fig. 3.2.2.

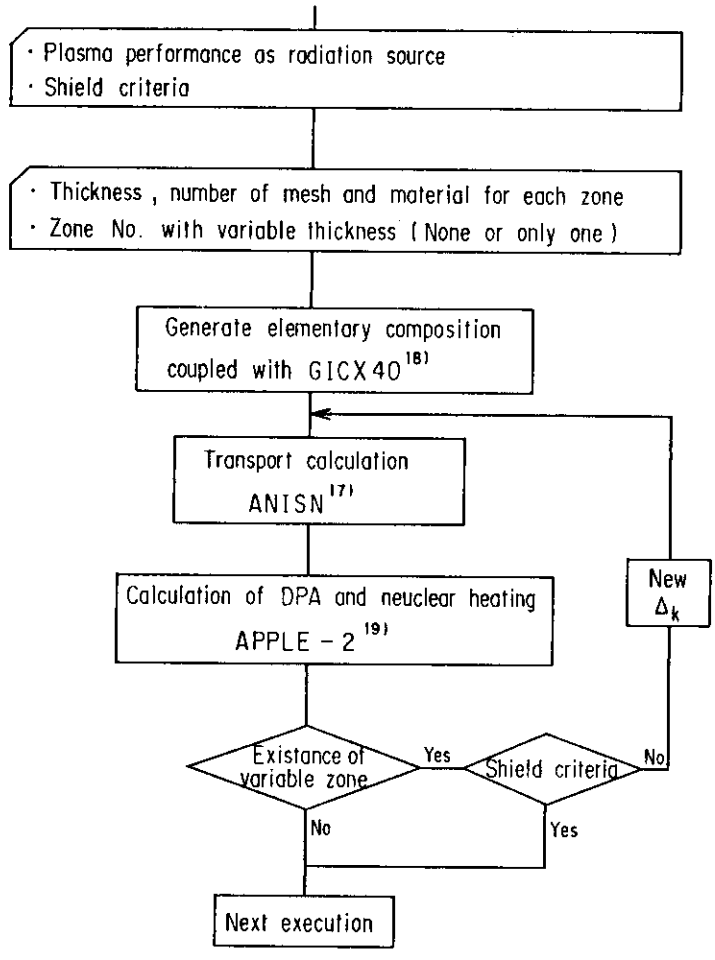

Fig. 3.2.2 Computation logic for shield design

3.3 Design of Toroidal Field (TF) Coil

3.3.1 Basic Consideration and Features

The TF coil geometry is determined to be consistent with the plasma performance objectives and the technical and geometrical constraints. The TF winding cross-sectional area is determined based on input values of maximum allowable current density and maximum allowable field and an allowable stress level in the coil. The field on plasma axis is resultantly obtained. The TF inner leg is sized based on the distance (Δ defined in Section 3.2) between a plasma surface and the TF coil conductor inside the torus, the plasma major and minor radii and the required volt-seconds supplied by PF coils. An iteration loop is available for adjusting the required volt-seconds. The outer leg is positioned based on the larger one of followings.

- o A minimum radius to accommodate the torus structures

or

- o A radius to limit the value of magnetic field ripple at the plasma surface to an acceptable value which is an input value

The TF coil shape is drawn automatically from the radial positions of the inner and outer legs. However in some options, an upper limit on the size is imposed by the requirement of plasma shaping by PF coils placed outside the TF coils and/or the maintenability of the torus structure.

3.3.2 Computation Logic and Option

In this routine, three types of TF coil shapes are available, which are the circular shape, the constant tension shape and the smooth Dee shape. The computation logic for determining the TF coil shape is shown in Fig. 3.3.1. The calculation flow is classified in three groups according to the plasma design flow option before listed in Table 3.1.3. The Group I includes the option No. 1, 3, 4 and 5. The Group II includes the option No. 2, 6, 7, 8, 9 and 10. The Group III includes the option No. 11, 12, 13.

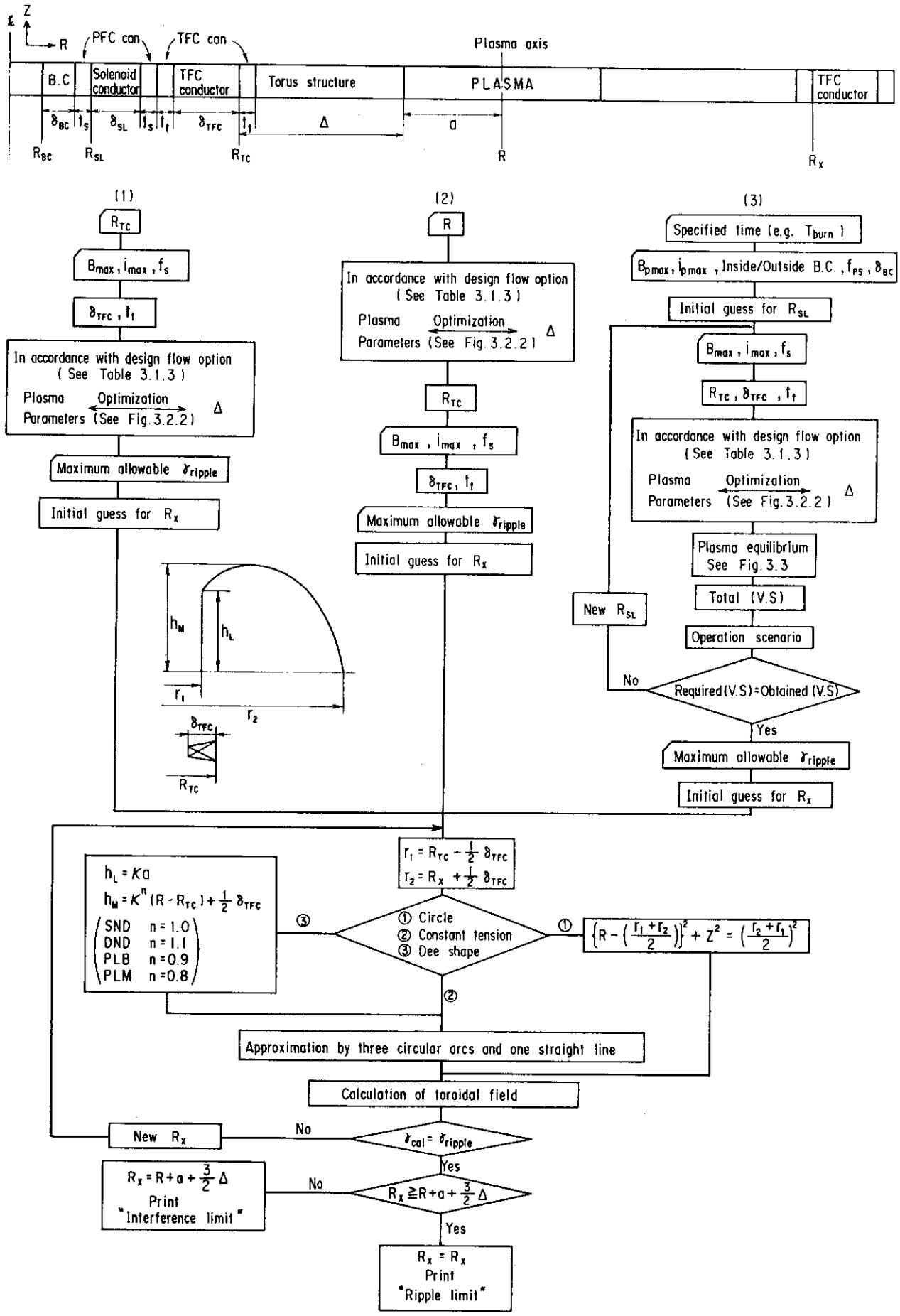

Fig. 3.3.1 Flowchart for computation of TF coil shape

Here, we describe i) the geometrical relationship in the TF coil winding cross-sectional area associated with maximum allowable field strength and maximum allowable current density, ii) the initial guess of the position of the TF coil outer leg, and iii) the approximated expression of the constant tension shape and the Dee shape.

i) TF coil winding cross-sectional area

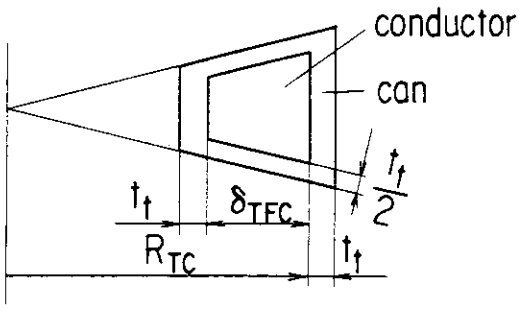

The input values are the maximum allowable field strength (B_{max}), the maximum allowable current density (i_{max}) and the space factor (f_s). The space factor is defined as conductor area/(conductor + can) area.

The TF coil ampere-turns I_{RF} is expressed as

$$I_{TF} = (2\pi R_{TC}/\mu_0)\, B_{max} \,. \tag{3.3.1}$$

The conductor thickness δ_{TFC} and the can thickness t_t are given by the following set of formulas.

$$i_{max}\{\pi(R_{TC}+t_t)^2 - \pi(R_{TC}-\delta_{TFC}-t_t)^2\}f_s = I_{TF} \tag{3.3.2}$$

$$\frac{\delta_{TFC}\{\,2\pi(\,R_{TC} - \frac{\delta_{TFC}}{2}\,) - Nt_t\}}{(\delta_{TFC}+2t_t)\{2\pi(R_{TC} - \frac{\delta_{TFC}}{2}\,)\}} = f_s \tag{3.3.3}$$

where, N is number of TF coils.

ii) Initial guess of the position of TF coil outer leg

The initial guess and the next guess in the iteration process are important for rapid convergence to a solution. In general, the calculation of magnetic field requires much CPU time. Therefore, we use the following formula expressing the field ripple for determining the provisional position of TF coil outer leg.

$$\gamma = \beta \left\{ \frac{1}{\left(\frac{r_p}{r_1}\right)^N - 1} + \frac{1}{\left(\frac{r_2}{r_p}\right)^N - 1} \right\} \quad 20) \qquad (3.3.4)$$

where

β : correction coefficient (β=1.5 is employed)

N : number of TF coils

r_1 : position of TF coil inner leg

r_2 : position of TF coil outer leg

r_p : plasma outer radius

Therefore, the next guess of r_2 (expressed by R_2) in the iteration process should be given by following equation.

$$\left\{ \frac{1}{\left(\frac{r_p}{r_1}\right)^N - 1} + \frac{1}{\left(\frac{R_2}{r_p}\right)^N - 1} \right\} \Big/ \left\{ \frac{1}{\left(\frac{r_p}{r_1}\right)^N - 1} + \frac{1}{\left(\frac{r_2}{r_p}\right)^N - 1} \right\} = \frac{\gamma_{ripple}}{\gamma_c} \qquad (3.3.5)$$

where, γ_{ripple} and γ_c are the maximum allowable ripple given as a input value and the calculated ripple, respectively. The formula (3.3.4) is based on a geometrical model shown in Fig. 3.3.2. Each filamentary current is extended infinitely.

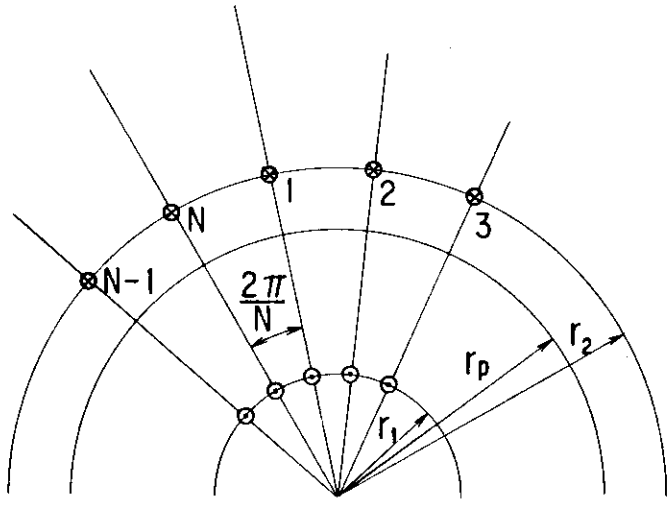

Fig. 3.3.2 Geometrical model for simplified ripple calculation

iii) Approximated expression of TF coil shape

In the case of circular shape, it is not necessary to approximate the TF coil shape. When the positions of the outer and inner legs are given, the TF coil shape is presented in R-Z space according to the following equation.

$$\left\{ R - \frac{r_1 + r_2}{2} \right\}^2 + Z^2 = \left(\frac{r_2 - r_1}{2} \right)^2 \qquad (3.3.6)$$

where, r_1 and r_2 are the R-positions of the inner and outer legs, respectively.

In the other cases (constant tension shape and Dee shape) however, it is useful for later design calculations to employ the patterned approximation which is carried out by the combination of the three circular arcs and one straight line as shown in Fig. 3.3.3.

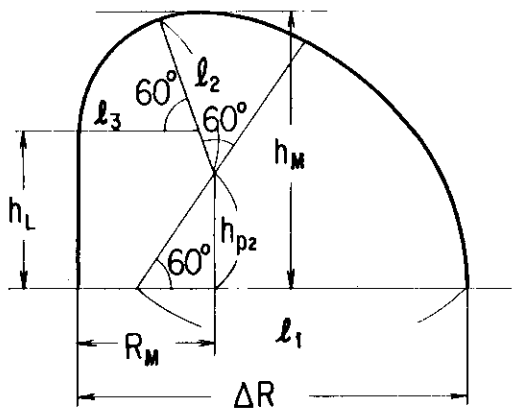

Fig. 3.3.3 Paterned aproximation of TF coil shape

ΔR : bore diameter in R-direction (r_2-r_1)

h_M : half of bore diameter in Z-direction

R_M : distance between inner leg and coil highest point in R-direction

h_L : half length of straight part

ℓ_i : radius of i-th circular arc

h_{p_2} : height of center of 2nd circular arc

When r_1 and r_2 are given, the constant tension shape is drawn automatically in accordance with the following equations,

$$Z = R_o k \{ e^{ku} \sqrt{1-u^2} + k \int_u^1 e^{kt} \sqrt{1-t^2}\, dt \}$$

$$R = R_o e^{ku} \qquad (3.3.7)$$

where,

$$R_o = \sqrt{r_1 r_2}$$

$$k = \frac{1}{2} \ell n \ (r_2/r_1)$$

$$-1 \leqq u \leqq 1$$

Furthermore, h_M and h_L are presented as follows.

$$h_M = R_o k \left\{ e^{ku\sqrt{1-u^2}} + k \int_u^1 e^{kt\sqrt{1-t^2}} \, dt \right\}\Big|_{u=0}$$

$$h_L = R_o k \left\{ e^{ku\sqrt{1-u^2}} + k \int_u^1 e^{kt\sqrt{1-t^2}} \, dt \right\}\Big|_{u=-1}$$

Therefore, h_{p^2}, ℓ_2, ℓ_1, ℓ_3 and R_M are presented as follows by using a condition of differential possibility at the connection points.

$$h_{p^2} = \frac{\sqrt{3}}{2(\sqrt{3}-1)} \left(2h_M - \frac{1}{\sqrt{3}} h_L - \Delta R\right)$$

$$\ell_2 = h_M - h_{p^2}$$

$$\ell_1 = \frac{2}{\sqrt{3}} h_{p^2} + \ell_2 \qquad (3.3.8)$$

$$\ell_3 = \frac{3}{\sqrt{3}} (h_{p^2} - h_L) + \ell_2$$

$$R_M = \frac{1}{2} (\ell_2 + \ell_3)$$

In the case of Dee shape, h_L and h_M can not be automatically calculated from only the given values of r_1 and r_2. Here we give h_L and h_M as follows.

$$h_L = \kappa \, a$$

$$h_M = \kappa^n (R - R_{TC}) + \frac{1}{2} \delta_{TFC} \qquad (3.3.9)$$

The n varies according to the variations of the impurity control system, which are single null divertor (SND), double null divertor (DND), pump limiter at bottom (PLB) and pumped limit at midplane. We assume n as follows.

SND　n = 1.0
DND　n = 1.1
PLB　n = 0.9
PLM　n = 0.8

3.4 Design of Poloidal field (PF) coil and MHD equilibrium

3.4.1 Basic consideration and Feature

The poloidal field (PF) coil system provides the necessary poloidal fields to maintain plasma equilibrium, the parameters of which vary widely during a operation phase. These fields can be split into an equilibrium part, which positions and shapes the plasma, and a part which drives the plasma current having a negligible stray field in the plasma region. The recent design of the PF coil system is however, of the hybrid type, i.e. most poloidal coils contribute both to the equilibrium field and to the plasma transformer field. A design optimization can be realized by revealing an interrelationship between plasma β, plasma cross-section, RF coil position and current programes.

3.4.2 Computation logic and Option

The key executions of PF coil design are to decide the geometrical arrangement of PF coil system and to calculate the required current for RF coil system, whose computation logic is shown in Fig 3.4.1.

i) Option of RF coils locatable region

Desirable coil locations (which minimize the total ampere turns) must also satisfy the space, access, shielding, and maintenance requirements. The choice of the PF coils being internal or external to the TF bore, is one of the key issues in the reactor concept. Outside PF magnets require large quantities of current and hence superconducting winding material. On the other hand, inside, i.e. linked, PF coils seem to lead to practically insurmountable problems for maintenance and repair of interior parts of the reactor.

Here, we limit the PF coils locatable region only external to the TF coil. We prepared four types of locatable regions as shown in Table 3.4.1. At first, the geometrical arrangement of many PF coils takes an uniform distribution in the locatable regions. After the MHD

equilibrium calculation with the uniform distribution, the number of RF coils reduces according to the manner of lumping, which will be described later.

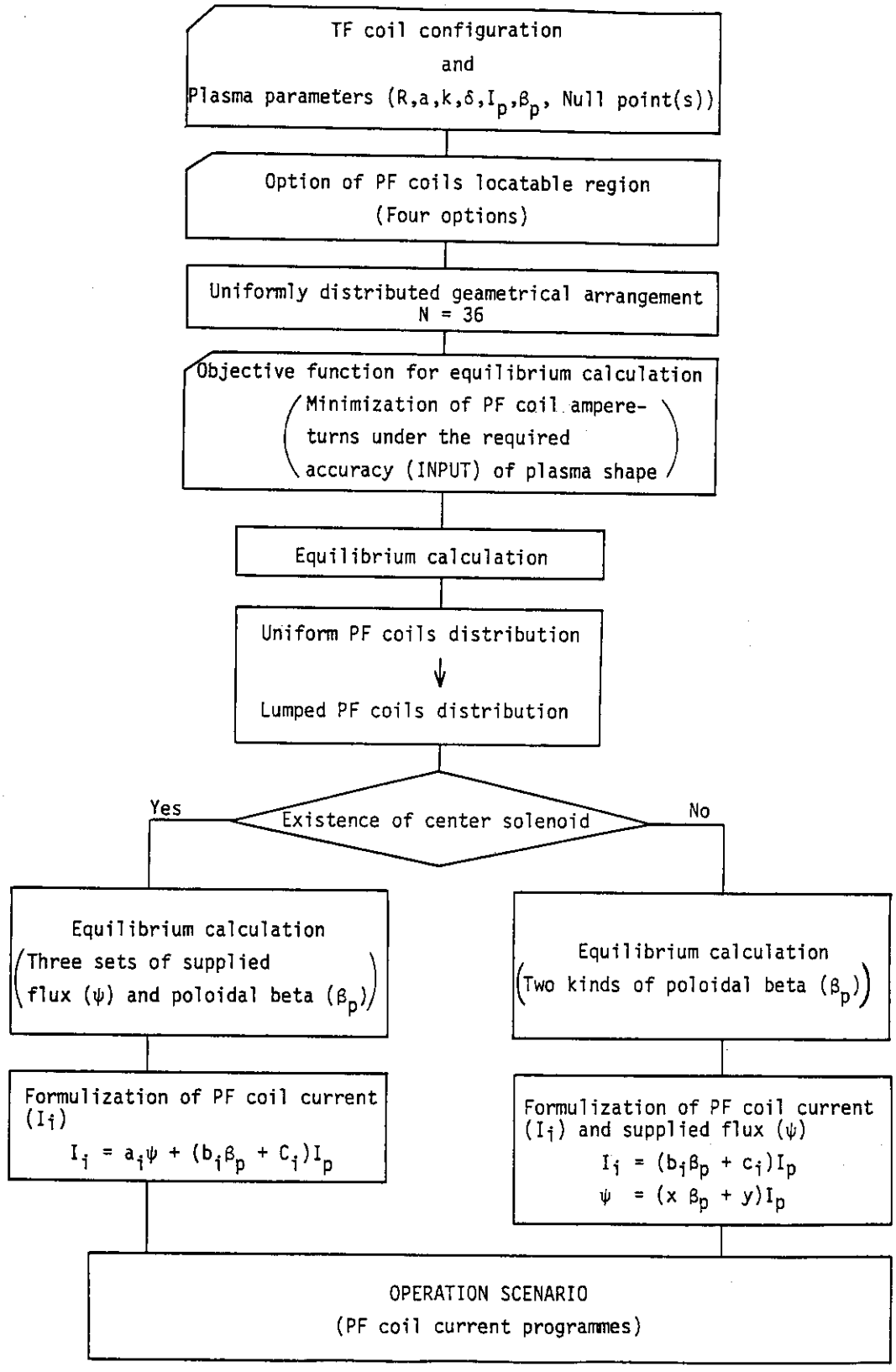

Fig. 3.4.1 Computation logic of PF coil location and current

Table 3.4.1 Option of PF coil locatable region
(shadow parts are forbidden regions)

Option 1	Option 2	Option 3	Option4
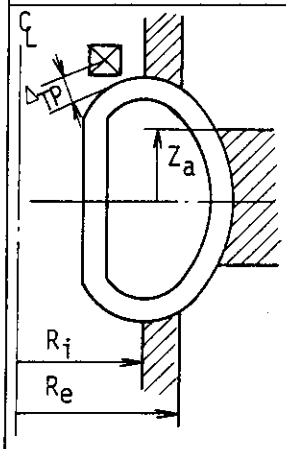	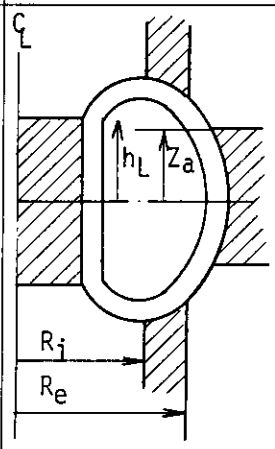	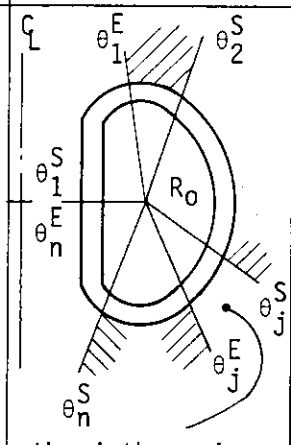 the j-th region	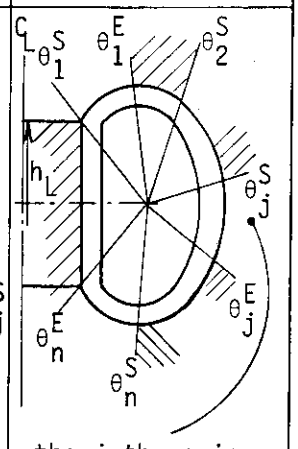 the j-th region
$R_i = R$ $R_e = R + a$ $Z_a = \kappa a + \Delta - t_t$ (see Fig. 3.3.1) h_L (see Fig. 3.3.1)		n : Number of locatable regions $\Delta\theta_j$: the j-th locatable region $\theta_j^S \leq \Delta\theta_j \leq \theta_j^E$ The actual values of n, θ_j^S and θ_j^E (j = 1, n) showld be given as input data.	

The distance between (Δ_{TP}) TF coil outer surface and center of PF coil is assumed as follows.

Solenoid region: $\Delta_{TP}^S = \begin{cases} \frac{\delta_{SL}}{2} + t_s & \text{(external to bucking cylinder)} \\ \frac{\delta_{SL}}{2} + ts + \delta_{BC} & \text{(internal to bucking cyclinder)} \end{cases}$

Other region : $\Delta_{TP}^O = \frac{\delta_{TFC}}{2} + t_t$ (See Fig. 3.3.1)

ii) MHD equilibrium calculation

In the axisymmetric toroidal system, the equilibrium magnetic field B and current J are written by the poloidal flux function $\psi(R,Z)$ in the cylindrical coordinates (R,Z,ϕ):

$$B = \nabla\phi \times \nabla\phi + F\nabla\phi \tag{3.4.1}$$

and

$$\mu_0 J = \Delta^*\psi\Delta\psi + \nabla F \times \nabla\psi \ , \tag{3.4.2}$$

where

$$\Delta^*\psi = R^2\nabla\cdot(\nabla\psi/R^2) = R\frac{\partial}{\partial R}\left(\frac{1}{R}\frac{\partial\psi}{\partial R}\right) + \frac{\partial^2\psi}{\partial Z^2} \ . \tag{3.4.3}$$

The equation for MHD equilibria, $P=\nabla J\times B$, can be reduced to the Grad-Shafranov equation,

$$\Delta^*\psi = -R^2\mu_0\frac{dP}{d\psi} - \frac{dF^2}{d\psi} = g(R,\psi) \quad \text{(in a plasma)} \tag{3.4.4a}$$

and

$$\Delta^*\psi = 0 \quad \text{(in a vacuum)} \ , \tag{3.4.4b}$$

when the plasma pressure is isotropic and is a function of ψ. The poloidal current function, $F(F=RB_t$, B_t:toroidal magnetic field) is also the function of ψ. The functions P and F are arbitrary in eq.(3.4.4). The time-evolution of these functions are determined by a transport process. For the MHD stability analysis, P and F are given by using a simple model e.g. functions of ψ.
The shape of a plasma surface is specified by the functions.

$$R = R_0 + a\cos + (\theta + \delta'\sin\theta) \ , \tag{3.4.5a}$$

and

$$Z = \kappa a \sin\theta \ , \qquad (3.4.5b)$$

where R_o, κ and a are the major radius of the plasma center, the ellipticity and the minor radius, respectively. The parameter, δ', specifies the triangularity. The solution of the equation, $\Delta^*\psi_\mu=0$, gives the poloidal magnetic flux supplied by external coils (vacuum field solution). The general solution, $\{\psi_{vj}\}$, are used to control a plasma phase. The vacuum flux is expressed by a linear combination of the general solutions:

$$\psi_v = \sum_{j=1}^{M} C_j \psi_{vj} \ . \qquad (3.4.6)$$

The coefficients, $\{C_i\}$, are determined so that the flux contour with $\psi+\psi_\mu=\psi_s$ may pass the specified points on the plasma surface given by eq.(3.4.5), (ψ:the solution of the Grad-Shafranov equation, ψ_s: flux at the plasma surface). The condition that the contour with $\psi+\psi_\mu=\psi_s$ passes the specified points is too stringent for the PF coil systems design. For this purpose, a least square error can be minimized:

$$E = \sum_i a_i \left|(\psi+\psi_v)_i-\psi_{si}\right|^2 + \sum_i b_i I_i^2 + c\ |\nabla\psi|^2_{mull} = \min^* \ , \qquad (3.4.7)$$

where $\{a_i\}$, $\{b_i\}$, c and I_i are the weights and the currents in the external coils. Minimization of E with respect to the variation, δI_i, leads to a linear simultaneous equation, $A\delta I=d$. The solution gives currents in external coils which fit the plasma surface to specified points with minimum least square error. Further conditions, e.g. the condition for total poloidal flux, can be introduced as the constraints to this equation.

Figure 3.4.2 shows the computation logic for obtaining the reasonable PF coils currents.

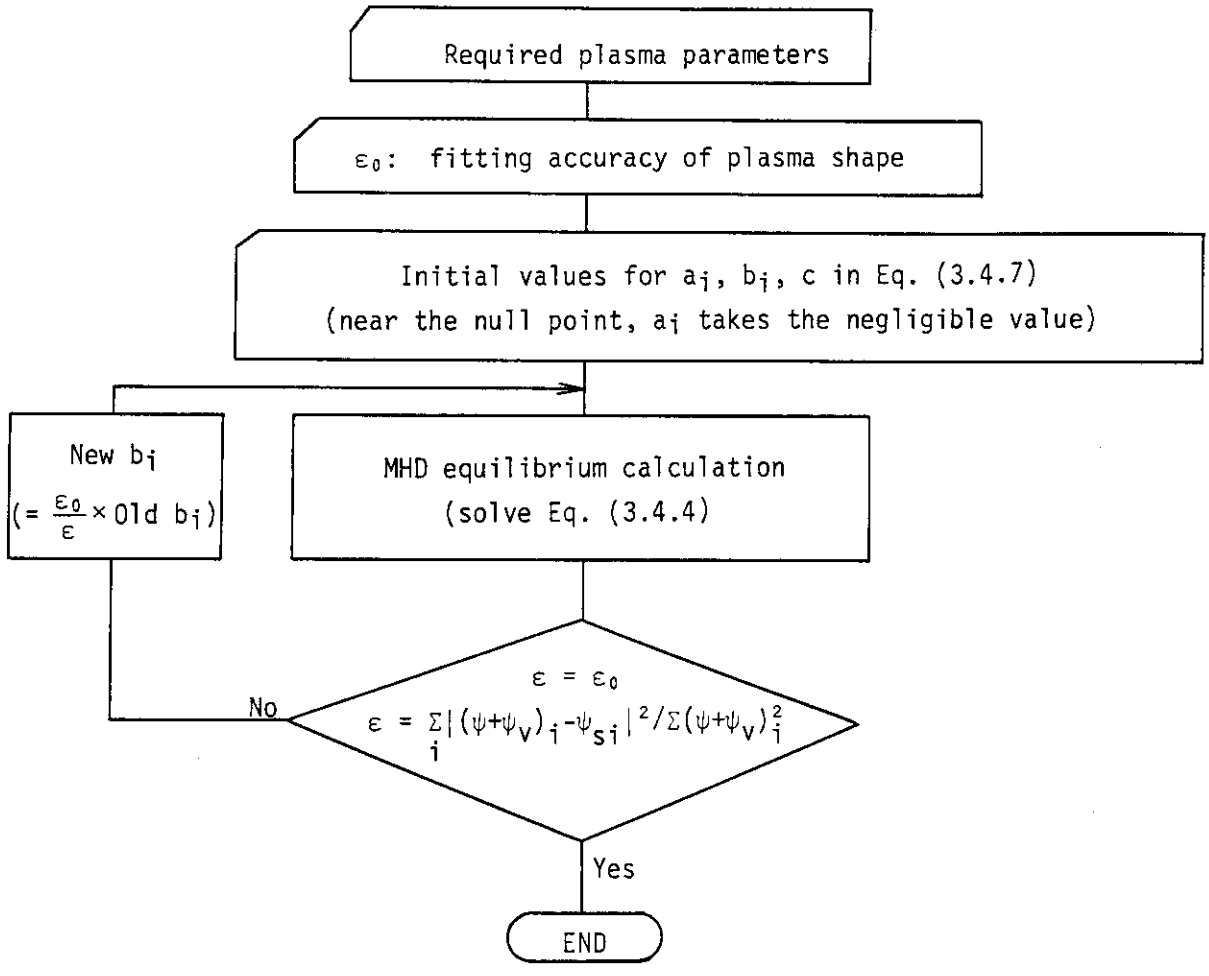

Fig. 3.4.2 Computation logic of MHD equilibrium calculation

iii) Manner of lumping the PF coils

At first, the geometrical arrangement of many PF coils takes an uniform distribution in the locatable regions. After the MHD equilibrium calculation with the uniform distribution, the PF coils number should be reduced to the reasonable number. If the MHD equilibrium is carried out with sufficiently many PF coils (e.g. NP), we will obtain the PF coil current distribution as shown in Fig. 3.4.3. When the required current in the k-th PF coil is denoted as I_k, the total ampere turns (AT) is represented as

$$AT = \sum_{k=1}^{ND} | I_k | .$$

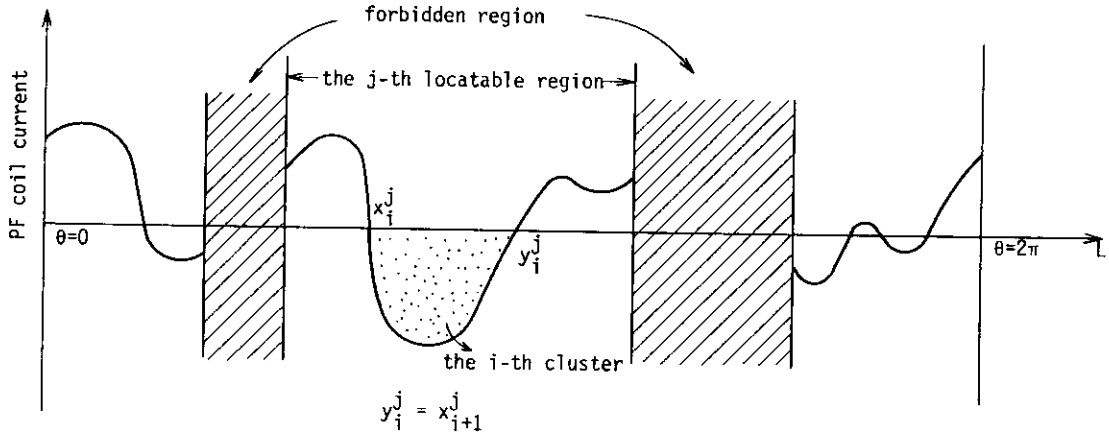

Fig. 3.4.3 Schematic picture of PF coil current distribution

Consequently, the following quantities can be clarified from Fig. 3.4.3.

Nrgn: number of locatable regions

Ncls: number of clusters in the i-th locatable region

NP : number of PF coils in the i-th cluster of the i-th locatable region ($NP=\sum_j \sum_i NP_i^j$)

AT : ampere turns in the i-th cluster of the i-th locatable region

$$AT = \sum_i \sum_i A\, T_i^j = \sum_{k=1}^{NP} |I_k|$$

$$AT_i^j = \sum_X^Y I_k$$

$$X = 1 + \sum_{\ell=1}^{j-1} \sum_i NP_i^\ell$$

$$Y = X - 1 + NP_i^j = NP_i^j + \sum_{\ell=1}^{j-1} \sum_i NP_i^\ell$$

Now, we can turn on the reduction of PF coils number. When the maximum allowable current in a single PF coil is denoted as I_{MAX}, we formularize the number of PF coils in the i-th cluster of the i-th locatable region as follow.

$$n_i^i = 1 + \text{Integer}\ (AT_i^j / I_{MAX})$$

In case of $n_i^j=1$, the coil position Z_i^j is represented as

$$Z_i^j = X_i^j + \frac{\int_{x_i^j}^{x_i^j} f_i^j \cdot L\, dL}{\int_{x_i^j}^{j_i^j} f_i^j \cdot dL} , \qquad (3.4.8)$$

where f_i^j is the fitting curve of the calculated current distribution in the concerned cluster.

In case of $n_i^j=2$, the coils positions $Z_i^j(1)$ and $Z_i^j(2)$ are represented as

$$Z_i^j(1) = x_i^j + \frac{\int_{x_i^j}^{x_i^j+z_i^j} f_i^j \cdot L \, dL}{\int_{x_i^j}^{x_i^j+z_i^j} f_i^j \, dL} \tag{3.4.9}$$

and

$$Z_i^j(1) = Z_i^j + \frac{\int_{x_i^j+z_i^j}^{y_i^j} f_i^j \cdot L \, dL}{\int_{x_i^j+z_i^j}^{y_i^j} f_i^j \, dL} \quad . \tag{3.4.10}$$

In case of $n_i^j=3$, the coils positions $Z_i^j(i)$, $Z_i^j(ii)$ and $Z_i^j(iii)$ are represented as

$$Z_i^j(i) = Z_i^j(1) \quad , \tag{3.4.11}$$

$$Z_i^j(ii) = Z_i^j \tag{3.4.12}$$

and

$$Z_i^j(iii) = Z_i^j(1) \quad . \tag{3.4.13}$$

In case of $n_i^j \geq 4$, the coils position are represented one after another as $x_i^j+\delta_i^j$, $x_i^j+2\delta_i^j$, ..., $x_i^j+(n_i^j-1)\delta_i^j$ and $x_i^j+n_i^j\delta_i^j=y_j^i-\delta_i^j$, where

$$\delta_i^j = \frac{y_i^j - x_i^j}{x_i^j + 1} \quad .$$

In consequence of lumping the PF coils, the total number of PF coils becomes $\sum_j \sum_i n_i^j$. The MHD equilibrium calculation should be carried out again with these resultant PF coil configuration.

iv) Formulization of the PF coil current as functions of supplied magnetic flux ψ, poloidal beta β_p and plasma current I_p.

The MHD equilibrium field consists of the dipole(vertical) field, the quadrapole field, the hexapole field and so on. All the fields components are in proportion to the plasma current and also are empirically found to be represented by the linear combination of the poloidal beta β_p. Therefore, the required current in the i-th PF coil can be represented as

$$I_i=(b_i\beta_p+C_i)I_p, \tag{3.4.14}$$

where b_i and C_i are the constants. By executing the equilibrium calculations in two different poloidal beta values, the unknown quantities b; and C_i are solved. The supplied flux(volt-seconds) ψ is represented as the linear combination of $I_k(k=1, \sum_j \sum_i n_i^j)$, so that we obtain the following furmula.

$$\psi = (x\beta_p+y)I_p \tag{3.4.15}$$

where the unknown values x and y are solved in the same manner of b_i and Ci solution.

On the other hand, when the PF coils are located also in the solenoidal region, the primary field(i.e. supplied volt-seconds) which has no effect upon the equilibrium configuration can be determined arbitrarily. Therefore, the required current in the i-th PF coil can be represented as

$$I_i=a_i\psi+(b_i\beta_p+C_i)I_p, \tag{3.4.16}$$

where $a_i b_i$ and C_i are the constants. By executing the equilibrium calculations in three different sets of (ψ, β_p), the unknown quantities a_i, b_i and C_i are solved.

4. Summary

We have described the calculation modes and formulae used in TRADE code, especially for the components (e.g. shield structure, TF coil system and PF coil system) closely related to the plasma column. Because the overall concept of the tokamak reactor might be almost identified by these components including the plasma performance and the operation scenario, the major effort was made for finding the optimum compromise between them. The design specifications of the auxiliary systems (e.g. power supply system, exhaust system cooling system cryogenic system, fuel system and etc.) are resultantly obtained. The design routines of the auxiliary systems are described in Ref. 2). The calculation results are examplified in JAERI-M 87-103 which is to be published one after another.

Acknowledgements

The authors would like to express their appreciation to Dr. K. Shinya for his fruitful comments on the plasma equilibrium calculation and to Dr. S. Mori for his helpful comments on the shield calculation. The authors also would like to express their appreciation to Drs. M. Sugihara, S. Yamamoto, H. Iida and N. Fujisawa for their continued encouragement.

4. Summary

We have described the calculation modes and formulae used in TRADE code, especially for the components (e.g. shield structure, TF coil system and PF coil system) closely related to the plasma column. Because the overall concept of the tokamak reactor might be almost identified by these components including the plasma performance and the operation scenario, the major effort was made for finding the optimum compromise between them. The design specifications of the auxiliary systems (e.g. power supply system, exhaust system cooling system cryogenic system, fuel system and etc.) are resultantly obtained. The design routines of the auxiliary systems are described in Ref. 2). The calculation results are examplified in JAERI-M 87-103 which is to be published one after another.

Acknowledgements

The authors would like to express their appreciation to Dr. K. Shinya for his fruitful comments on the plasma equilibrium calculation and to Dr. S. Mori for his helpful comments on the shield calculation. The authors also would like to express their appreciation to Drs. M. Sugihara, S. Yamamoto, H. Iida and N. Fujisawa for their continued encouragement.

References

1) M. Kasai, et al., "The Sensitivity Study Code for Tokamak Devices" Proceeding of 9th Symposium on Engineering Problems of Fusion Research, Vol. 2, P1880, Chicago, Illinois, October 26-29, 1981.
2) S. Nishio, et al., "Development of Tokamak Reactor System Analysis Code (TORSAC)" JAERI-M 87-021 (1987).
3) M. Sugihara, et al., "Plasma Design Consideration of Near Term Tokamak Fusion Experimental Reactor" J. of Nucl. Sci. and Technol., Vol. 19, No. 8, Aug. 1982, 628-637.
4) T. Tuda, et al., "Accessible beta value of Tokamak" 10th Int. National Conf. on Plasma Phys. and Controlled Nucl. Fusion Research, London, UK, 1984.
5) M. Murakami, et a., "Some Observation on Maximum Densities in Tokamak Experiments" Nucl. Fusion 16 (1976) 347.
6) L.C. Bernard, R.W. Moore, Phys. Rev. Lett 46 (1981) 1286
7) F. Troyon, et al., Plasma Phys. 26 (1984) 209.
8) V.S. Mukhvatov, V.U. Shafranov, "Plasma Equilibrium in a Tokamak" Nucl. Fusion 11, (1971) 605.
9) K. Miyamoto, "Plasma Physics for Nuclear Fusion" The MIT Press (1980), Cambridge, Massachsetts, and London, England.
10) M.D. Kurskal, et al., Phys. of Fluids 1 (1958) 321.
11) G. Laval, et al. "Equilibre, Stabilite at Diffusion Dun Plasma Torique a Section Transversale non Circulaire" Plasma Phys. and Controlled Nucl. Fusion Research", 2, (1971), 507 IAEA, Vienna
12) J.F. Clarke, Nucl. Fusion 20 (1980) 563.
13) D.R. Sweetman, "Ignition Condition in Tokamak Experiments and Role of Neutral Injection Heating", Nucl. Fusion, 13, (1973), 157.
14) D.M. Himmelblan, "Applied Nonlinear Programming", McGraw-Hill Book Conpany (1979).
15) J.A. Nelder, R. Mead, "A Simplex Method for Function Minimization", Computer J., 11 (1968) 302.
16) K. Horigami, et al., "A Program Package for Solving Nonlinear Optimization Problems: User's Manual" JAERI-M 9154 (1980)
17) W.W. Engle, Jr., "A users manual for ANISN, a One-dimentional Discrete Ordinates Transport Code with Anisotropic Scattering"

Computing Technology Center, Vnion Carbide Corporation, K-1693 (1976).

18) Y. Seki, H. Iida, "Coupled 42-Group Neutron and 21-Group Gamma Ray Cross Section Set for Fusion Reactor Calculation" JAERI-M 8818 (1980).

19) H. Kawasaki, Y. Seki, "APPLE-2: An Inproved Version of APPLE Code for Plotting Neutron and Gamma Ray Spectra and Reaction Rates "JAERI-M 82-091 (1982).

20) T. Hiraoka, et al., "Conceptual Studies of Plasma Engineering Test Facility" JAERI-M 8198 (1979).